MATHEMATICAL MODEL FOR MANOEUVRING OF TWIN-PROPELLER TWIN-RUDDER SHIP CONSIDERING PECULIAR RUDDER NORMAL FORCE PHENOMENON

Sahbi Khanfir (Kobe University, Japan)
Kazuhiko Hasegawa (Osaka University, Japan)
Ei-chi Kobayashi (Kobe University, Japan)
Vishwanath Nagarajan (Indian Institute of Technology, Kharagpur, India)

Abstract: MMG model is well known as a mathematical model for ship manoeuvrability. Although it is originally established for single-propeller single-rudder ships, some researchers have attempted and succeeded to expand it for other types of ships. However, it is still very hard to estimate the hydrodynamic coefficients, especially interaction coefficients, without conducting model experiments. Furthermore, conventional empirical formulae to estimate them such as Kijima's regression model are not properly suitable for non-conventional ships, because of lack of sufficient mother data. Additionally, the flow field differs widely between single-propeller single-rudder and twin-propeller twin-rudder ships from various viewpoints, especially with respect to hydrodynamic interactions between hull, propeller and rudder. In this paper, the assessment of mathematical model for manoeuvring of twin-propeller twin-rudder ship is discussed. The effect of drift angle at cruising speed on the rudder forces and some peculiar phenomena concerning rudder normal force for twin rudder ships will be evaluated. A new method for estimating the hull-rudder interaction coefficients based on free-running experimental results will be proposed.

1. INTRODUCTION

Mathematical model for ship manoeuvrability is the most important issue for a ship manoeuvring simulation. From the viewpoints of ship manoeuvrability, when checking the ship's manoeuvring characteristics according to the manoeuvring standards, several methods are being used such as the method based on a database, the method based on model test experimental data and the method based on numerical simulations using a mathematical model. For single-propeller single-rudder ships, manoeuvring ability has been extensively investigated [1], and useful conclusions were achieved by comparing model or full-scale tests with simulations using mathematical models. However there are not yet well-established models for twin-propeller twin-rudder ships as there are for single-propeller single- rudder ships. In fact, some theoretical and experimental researches have been directed to investigate the manoeuvring ability of the wide beam ships fitted with twin-rudder systems from various viewpoints [2,3]. Lee et al. [4,5] carried out Circular Motion Tests (hereinafter referred as "CMT") and free-running experiments on a wide-beam shallow-draft TPTR ship. They extended the applicability of the MMG model to TPTR ships. Indeed, they modified the mathematical model of the propeller wake fraction for a TPTR ship based on experimentally determined characteristics of the propeller wake. They concluded that the most important parameters in the TPTR ship are the propeller's effective wake during manoeuvring, and the flow-straightening coefficient of the rudder in both left and right turning of the ship. They could prove the validity of the new model for their typical subject ship by comparing the simulations with the free-running tests. Yoshimura and Sakurai [6] studied the manoeuvring characteristics of conventional and wide-beam TPTR ships at different water depths. The mechanism of shallow water effects on rudder force and hull force was investigated. It was shown that some TPTR ships could differ significantly in turning and course-keeping qualities from conventional ships in shallow water. The study concluded that the MMG-type mathematical model is also suitable for a TPTR ship, and a model with all the hydrodynamic coefficients for deep and shallow water was provided. Kim et al. [7] investigated the manoeuvring characteristics of a twin-propeller twin-rudder container ship and compared the hydrodynamic coefficients and the simulation results with those of a container ship fitted with single-propeller single-rudder ship. In this research, the mathematical model for manoeuvring of a twin-propeller twin rudder ship will be investigated. The effect of drift angle at cruising speed on the rudder forces and some peculiar phenomena concerning normal rudder force for twin-rudder ships are evaluated. A method to estimate the hull-rudder interaction coefficients based on free-running experimental results is proposed. Various parameters

included in the mathematical model for manoeuvring motion are investigated experimentally. The manoeuvring motion of twin-rudder ships is compared with free-running test results in order to examine the validity of the abovementioned procedures.

2. SUBJECT SHIP AND EXPERIMENTAL FACILITIES

2.1 Subject Ship:

One twin-propeller twin-rudder model-scale ship was used for this study. The principal particulars of the subject ship are shown in Table I.

Table I Subject ship principal particulars

Particulars	Subject ship
Hull	
L (m)	4.00
B (m)	0.85
d (m)	0.28
Trim(m)	0.00
LCG/L	-0.006
C_B	0.80
S_W (m^2)	4.9864
Propeller	
D_P (m)	0.136
P (m)	0.09724
Number of blades	4
$y_{P(S)}, -y_{P(P)}$ (m)	0.14
Scale ratio	1/16.00

The model ship was used to compare the simulation results with the values measured during free-running experiments. She was also used to validate the new prediction method mentioned above. The subject ship is fitted with a bow thruster. During all captive model tests as well as free-running experiments, the bow thruster tunnel is kept open. The stock propeller of IHI Corporation [8] (hereinafter referred as "IHI") was used for the model ship. The particulars of the stock propeller are shown in Table I. The subject ship was fitted with a conventional-type spade rudder. The layout of the twin-rudder system is shown in Fig. 1.

Fig. 1 Side view and stern view of the twin-propeller twin-rudder system for the subject ship

2.2 Experimental facilities

The captive model tests and the free-running experiments of the subject ship were conducted within the sea-keeping and manoeuvring tank of IHI. During resistance and self-propulsion experiments, to measure the forces and moment on the rudder, ship and propeller thrust strain gauge-type transducers were used. The propeller torque was measured using a magnetostrictive torque sensor. The resistance and self-propulsion tests are for model-free conditions (free to sink and trim) and were carried out using standard towing tank procedures. The experiment set up during the circular motion test (CMT) is shown in Fig. 2.

Fig. 2 View from forward of the subject ship fitted on the turntable during the CMT

3. EQUATIONS OF MANOEUVRING MOTIONS

In this research, an MMG-type mathematical model is used to investigate the manoeuvring characteristics of the twin-propeller twin-rudder model ship.
A three degree-of-freedom (surge, sway, and yaw) model is considered for the ship's manoeuvring motions. The coordinate system is shown in Fig. 3.

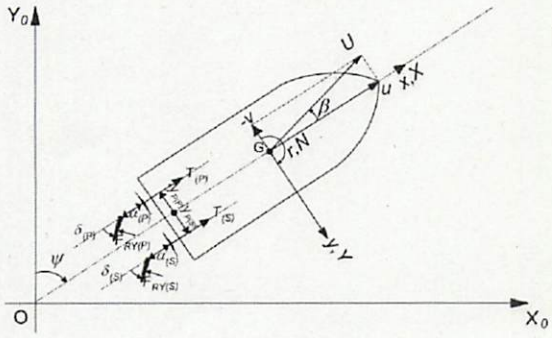

Fig. 3 Coordinate system

The equations of surge, sway, and yaw motion considering the origin of the coordinate system located at the ship's centre of gravity can be written as follows in Eq. 1.

$$\begin{aligned}(m+m_x)\dot{u}-(m+m_y)vr &= X_H+X_P+X_R\\ (m+m_y)\dot{v}+(m+m_x)ur &= Y_H+Y_P+Y_R\\ (I_{zz}+J_{zz})\dot{r} &= N_H+N_P+N_R\end{aligned} \quad (1)$$

The subscripts 'H', 'P' and 'R' refer to hull, propeller and rudder respectively. For a twin-propeller twin-rudder ship, there is the need to use sway and yaw terms (and) in the propeller mathematical model, which are due to the sway force and moment generated by both propellers as they are physically offset from the ship's centreline.

4. MANOEUVRING MATHEMATICAL MODEL OF TWIN-PROPELLER TWIN-RUDDER SHIP

A series of captive model tests were carried out to establish the TPTR ship's characteristics. The analysis of the experimental results is based on the MMG mathematical modelling procedure and various parameters, such as the propeller's effective wake, thrust deduction factor, and neutral rudder angle, which were investigated.

4.1 Hydrodynamic hull coefficients:

The mathematical model for hull forces and moment is defined as follows in Eq. 2.

$$\left.\begin{aligned}X_H &= \frac{1}{2}\rho LdU^2\begin{pmatrix}X'_0+X'_{|v|}|v'|+X'_{|r|}|r'|+X'_{vv}(v')^2\\ +X'_{vr}v'r'+X'_{rr}(r')^2\end{pmatrix}+\frac{1}{2}\rho S_R u^2 R'(u)\\ Y_H &= \frac{1}{2}\rho LdU^2\begin{pmatrix}Y'_0+Y'_v v'+Y'_r r'+Y'_{vvv}(v')^3+\\ Y'_{vvr}(v')^2 r'+Y'_{vrr}v'(r')^2+Y'_{rrr}(r')^3\end{pmatrix}\\ N_H &= \frac{1}{2}\rho L^2 dU^2\begin{pmatrix}N'_0+N'_v v'+N'_r r'+N'_{vvv}(v')^3+\\ N'_{vvr}(v')^2 r'+N'_{vrr}v'(r')^2+N'_{rrr}(r')^3\end{pmatrix}\end{aligned}\right\} \quad (2)$$

CMT experiments for the bare hull ship were conducted at the sea-keeping and manoeuvring tank of IHI and the least square method was used to calculate the hull coefficients. The non-dimensional hydrodynamic derivatives of bare hull are shown in Table II.

Table II Hydrodynamic derivatives of the bare hull of the subject ship

	X′		Y′		N′
X_0'	-0.021	Y_0'	-0.0016	N_0'	0.0007
$X_{\|v\|}'$	-0.0104	Y_v'	-0.2091	N_v'	-0.1641
$X_{\|r\|}'$	-0.0023	Y_r'	0.0144	N_r'	-0.0162
X_{vv}'	0.0679	Y_{vvv}'	-0.5195	N_{vvv}'	0.0096
X_{vr}'	-0.1884	Y_{rrr}'	-1.0971	N_{rrr}'	-1.168
X_{rr}'	-0.2163	Y_{vvr}'	-3.0849	N_{vvr}'	-3.6904
		Y_{vrr}'	-3.7333	N_{vrr}'	-4.106

4.2 Resistance of Ship:

The resistance of the ship model was measured for the bare-hull ship condition. The Prohaska method [9] was used in order to determine the resistance characteristics of the subject model ship C. $1+k$ is obtained by intercepting the straight line on the ordinate axis when Fn^4/C_{F0} is used as abscissa as shown in Fig. 4.

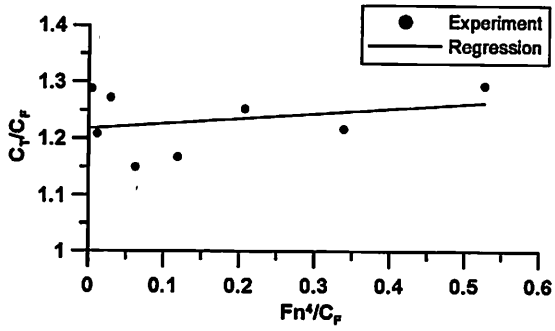

Fig. 4 Prohaska's method for determining the form factor of the subject ship

The measured resistance coefficient of the ship is shown in Fig. 5.

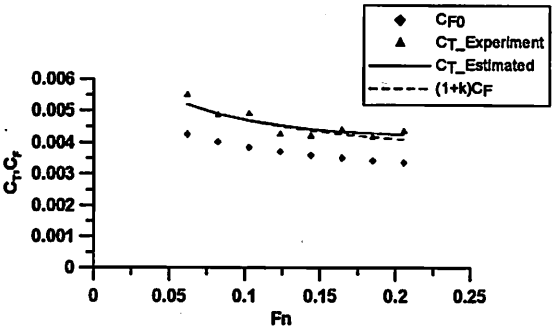

Fig. 5 Resistance coefficient of the subject ship

4.3 Mathematical model of propeller:

The hydrodynamic forces due to the propeller can be expressed as shown in Eq. 3. Fixed-pitch propellers were used and modelled in the present study. The resultant propeller sway force due to both propellers was considered insignificant, and was therefore neglected for this paper.

$$\left.\begin{aligned} X_P &= \rho\left\{\begin{matrix}(1-t_{P(S)})n_{(S)}{}^2 D_{P(S)}{}^4 K_{T(S)}(J_{P(S)})+\\ (1-t_{P(P)})n_{(P)}{}^2 D_{P(P)}{}^4 K_{T(P)}(J_{P(P)})\end{matrix}\right\} \\ N_P &= \rho\left\{\begin{matrix}(1-t_{P(S)})y_{P(S)}n_{(S)}{}^2 D_{P(S)}{}^4 K_{T(S)}(J_{P(S)})+\\ (1-t_{P(P)})y_{P(P)}n_{(P)}{}^2 D_{P(P)}{}^4 K_{T(P)}(J_{P(P)})\end{matrix}\right\} \end{aligned}\right\} \quad (3)$$

In Eq. 3, inside the parenthesis, the character "S" refers to starboard propeller and the character "P" to the port propeller respectively. This method of writing the equations for twin-propeller twin-rudder ship will be followed in the rest of the paper.

4.3.1 *Effective wake-fraction for propeller inflow in straight-running*

The thrust coefficients for the experiment $K_{TM_{(P)}^{(S)}}$ were calculated from the measured thrusts $T_{M_{(P)}^{(S)}}$ respectively for starboard and port propeller as shown in Eq. 4.

$$K_{TM(S)\,(P)} = T_{M(S)\,(P)} / \rho n_{(S)\,(P)}{}^2 D_{(S)\,(P)}{}^4 \quad (4)$$

With $K_{TM_{(P)}^{(S)}}$ as input data, the propellers' advance coefficient $J_{P_{(P)}^{(S)}}$ is read off from the propeller open-water chart. Effective wake-fraction coefficient for propellers' inflow in straight-running $w_{P0_{(P)}^{(S)}}$ was calculated using Eq. 5, and is shown in Fig. 6. $w_{P0_{(P)}^{(S)}}$ was formulated function of the advance ratio $J_{S_{(P)}^{(S)}}$.

$$1 - w_{P0(S)\,(P)} = \frac{J_{P(S)\,(P)} D_{P(S)\,(P)} n_{(S)\,(P)}}{U} \quad (5)$$

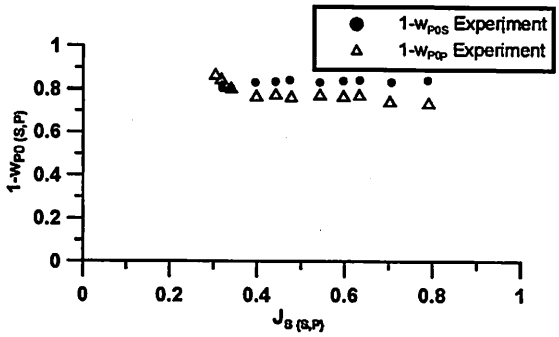

Fig. 6 Effective wake-fraction coefficients for starboard and port propeller inflow in straight-running of the subject ship

4.3.2 *Thrust deduction factor in straight-running*

The method of estimating the coefficient t_{P0} by the "conventional method" is shown in Eq. 6.

$$1 - t_{P0} = \frac{(R_{ua})_{Hull+rudder} - (SFC)_{Hull+rudder}}{(T)_{Hull+rudder}} \quad (6)$$

For the "proposed method," suggested by Toda, [10] since the rudder is not fitted on the model during resistance experiments, the method of estimating the coefficient t_{P0} is modified as shown in Eq. 7.

$$1 - t_{P0} = \frac{(R_{ua})_{Hull} - (SFC)_{Hull} + (X_R)_{Rudder\ behind\ propeller}}{(T)_{Hull+rudder}} \quad (7)$$

The variation of the thrust-deduction factor in straight-running is shown in Fig. 7.

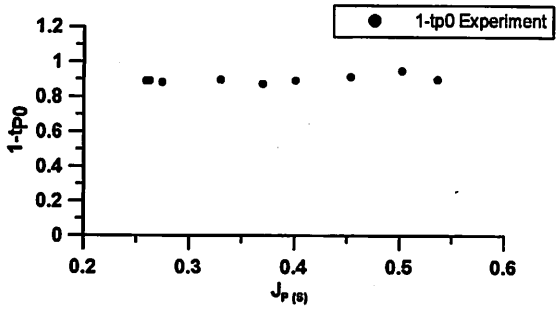

Fig. 7 Variation of the thrust-deduction factor in straight-running of the subject ship

In this study, the interaction coefficients of the subject ship will be compared with other twin-propeller twin-rudder ships. The comparison of principal particulars of subject ship and other reference ships is shown in Table III.

Table III Comparison between the principal particulars and lateral distance between the rudders and propellers of TPTR model ships

	L/B	B/d	$y_{P(S)}/B$	C_b
Subject ship	4.70	3.02	0.16	0.80
Heavy cargo carrier[4,5]	3.90	7.79	0.20	0.77
Conventional TPTR[1] ship[6]	5.44	3.60	0.15	0.75
Wide-beam TPTR ship[6]	3.70	5.35	0.28	0.80
Wide container[7]	7.10	3.40	0.15	0.67

The variation of the coefficients $W_{P0(P)}^{(S)}$ and t_{P0} function of principal particulars of twin-propeller twin-rudder ships are shown in Figs 8,9,10 and 11. The variations show quite similar trends for both coefficients in all the cases.

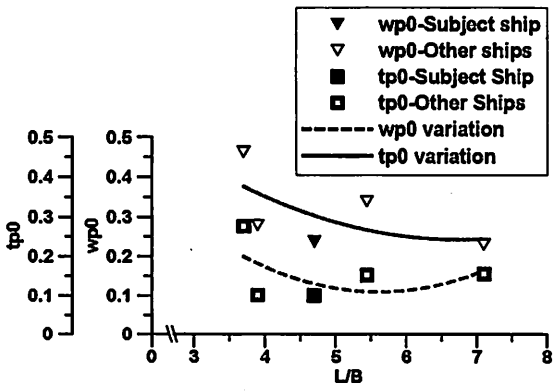

Fig. 8 Variation of tp_0 and w_{P0} function of Ship's length by ship's breadth ratio of TPTR ships

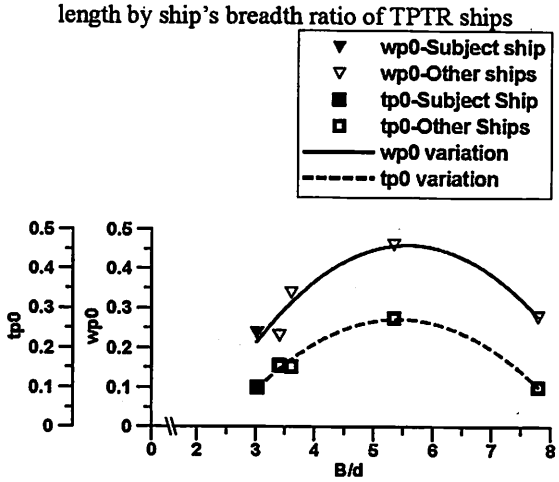

Fig. 9 Variation of tp_0 and w_{P0} function of ship's breadth by ship's draft ratio of TPTR ships

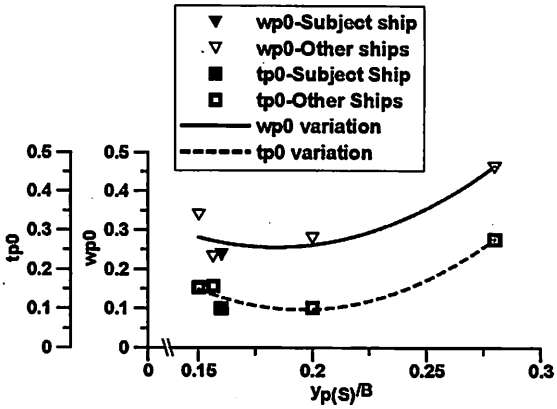

Fig. 10 Variation of tp_0 and w_{P0} function of lateral distance between starboard propeller and ship's centreline by ship's breadth ratio of TPTR ships

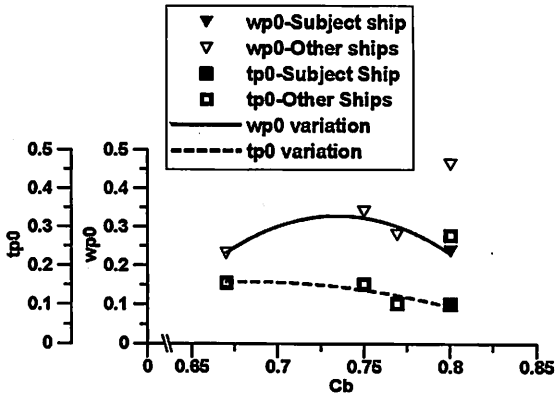

Fig. 11 Variation of tp_0 and w_{P0} function of ship's block coefficient of TPTR ships

4.3.3 *Increment of effective wake-fraction for propeller inflow in drift condition*

Several CMT experiments with propeller rotation were carried out in order to analyse the performance

[1] TPTR: twin-propeller twin-rudder

of the propeller in drift condition. To calculate the effective wake-fraction coefficient for propeller inflow in drift condition, the same method of analysis as for straight-running is used. The calculated increment of effective wake-fraction coefficient in drift condition $1-w_{P0_{(P)}(S)}$ is shown in Fig. 12. It was formulated as a function of $v^*_{P_{(P)}(S)}$, which is defined in Eqs. 8 and 9.

$$v'_P = -\sin\beta + x_P' r' \tag{8}$$

$$v^*_{P_{(P)}(S)} = v'_P + \tan^{-1}(y_{P_{(P)}(S)} / x_P) \tag{9}$$

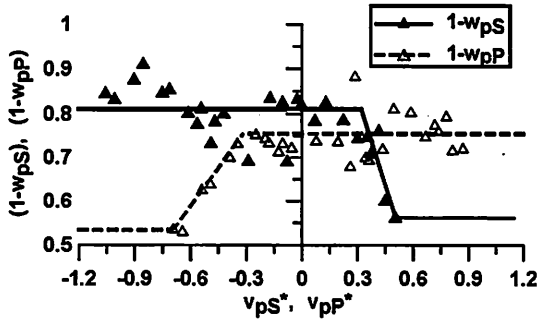

Fig. 12 Variation of the effective wake-fraction of the starboard and port propeller of the subject ship

The variation of the effective wake-fraction during manoeuvring regarding the twin-propeller twin-rudder ship is quite different when compared to that of the single-propeller single-rudder ship. The variation seems to be asymmetric concerning the starboard and port propeller for starboard and port turning, respectively. It is reported that the coefficient $w_{P_{(P)}(S)}$ will either decrease asymmetrically [4,5] or remain steady [6] regarding the twin-propeller twin-rudder system during manoeuvring motions. For the subject ship, the coefficient $w_{P_{(P)}(S)}$ is found to either remain steady or increase linearly.

4.4 Mathematical model of rudder:

The forces and moment due to the twin-propeller twin-rudder ship is expressed as shown in Eq.10.

$$\left.\begin{aligned} X_R &= -(1-t_{R(S)})(F_{RY(S)}\sin\delta_{(S)} + F_{RY(P)}\sin\delta_{(P)}) \\ Y_R &= -(1+a_H)(F_{RY(S)}\cos\delta_{(S)} + F_{RY(P)}\cos\delta_{(P)}) \\ N_R &= -(x_R + a_H x_H)(F_{RY(S)}\cos\delta_{(S)} + F_{RY(P)}\cos\delta_{(P)}) + f(x_R) \\ f(x_R) &= -y_{R(S)}(1-t_{R(S)})(F_{RY(P)}\sin\delta_{(P)} - F_{RY(S)}\sin\delta_{(S)}) \\ t_{R(S)} &= t_{R(P)} \end{aligned}\right\} \tag{10}$$

The detailed description of the mathematical model of the twin-rudder system was already deeply investigated [1,2] .

4.4.1 *Interaction between ship and rudder*

Several sets of experiments were carried out with different rudder angles and by fixing the ship's drift angle at 0 degrees in order to determine the interaction between the ship and the rudder. The ship's speed was set as = 0.643m/s, rps = 7.97, which corresponds to the actual ship's operating speed (5 knots).
To obtain the coefficients of the interaction between the hull and the rudders (t_R, a_H, x_H), the measured data were analyzed based on Eq. 10, and their values are shown in Table IV.

Table IV Ship-rudder interaction coefficients

t_R	0.2578
a_H	0.2877
$x_{H\,/L}$	-0.3719

The ship-rudder interaction coefficients of subject ship were compared with those of other twin-propeller twin-rudder ships that are listed out in Table III. The variations of the coefficients (t_R, a_H, x_H) function of principal particulars of twin-propeller twin-rudder ships are shown in Figs 13, 14, 15 and 16.

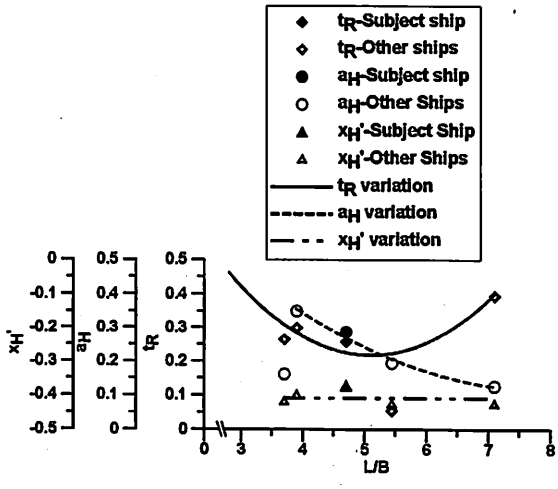

Fig. 13 Variation of (t_R, a_H, x_H) function of Ship's

length by ship's breadth ratio of TPTR ships

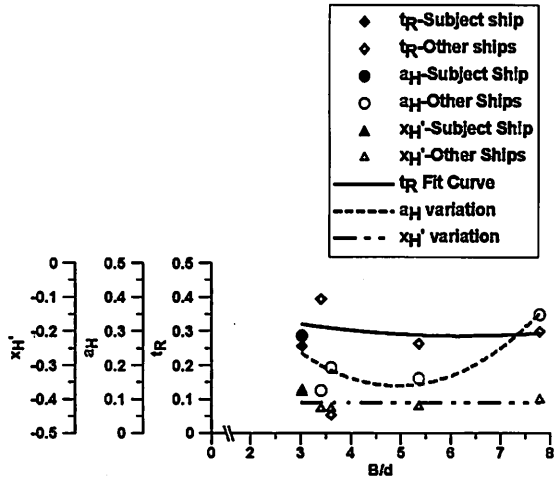

Fig. 14 Variation of (t_R, a_H, x_H) function of ship's breadth by ship's draft ratio of TPTR ships

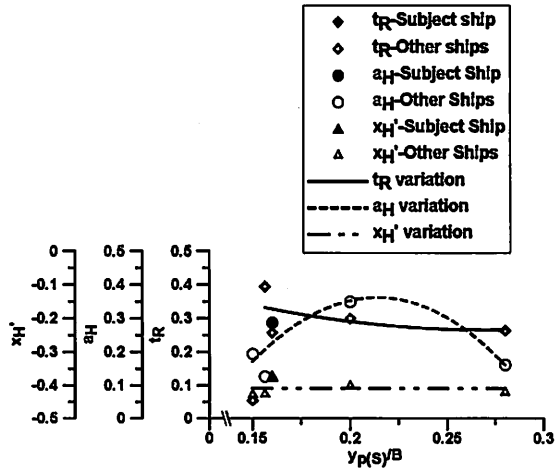

Fig. 15 Variation of (t_R, a_H, x_H) function of lateral distance between starboard propeller and ship's centreline by ship's breadth ratio of TPTR ships

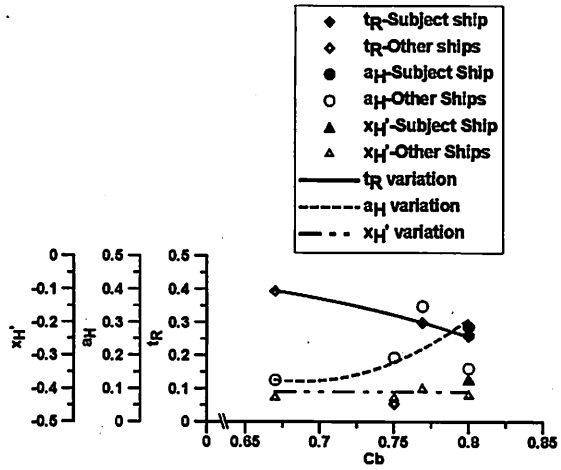

Fig. 16 Variation of (t_R, a_H, x_H) function of ship's block coefficient of TPTR ships

The coefficient x_H has almost constant value regardless the principal particulars of twin-propeller twin-rudder ships. The coefficient of reduction of rudder's resistance in ship's surge direction t_R seems to have a slight variation as compared with x_H's one. Whereas a_H has the most noticeable variation especially with respect to ships' block coefficients. Interestingly, the variation of a_H with respect to ships' block coefficients for twin-propeller twin-rudder ships shows a similar trend with the one for single-propeller single rudder ships [1].

4.4.2 *Estimation of flow-straightening related coefficients*

The effective inflow angle to the rudder for the twin-propeller twin-rudder system is expressed as shown in Eq. 11.

$$\underset{(P)}{\alpha_{R(S)}} = \underset{(P)}{\delta_{(S)}} - \underset{(P)}{\delta_{R(S)}}(\underset{(P)}{\beta_{R(S)}}) \tag{11}$$

The offset of the rudder from the ship's centreline is included in the effective rudder angle expression as shown in Eq. 12.

$$\underset{(P)}{\delta_{R(S)}} = \underset{(P)}{\gamma_{R(S)}}\,\underset{(P)}{\beta_{R(S)}} + \tan^{-1}\left(\underset{(P)}{y_{R(S)}} \Big/ \underset{(P)}{x_{P(S)}}\right) \tag{12}$$

The effective drift angle at rudder position is defined as shown in Eq.13.

$$\underset{(P)}{\beta_{R(S)}} = \beta - \underset{(P)}{L'_{R(S)}}\, r' \tag{13}$$

The inflow velocity in the sway direction to the rudder for twin-propeller twin-rudder model can be

expressed as shown in Eq. 14.

$$v_{R(S)} = u_{R(S)} \tan(\delta_{R(S)}) \quad (14)$$
$$(P) \qquad (P) \qquad (P)$$

Conventionally, the flow straightening coefficient is determined from captive model tests (Oblique towing test, CMT). In this research, the procedure to determine $L_{R_{(P)}(S)}$ and $\gamma_{R_{(P)}(S)}$ from free-running experiments will be described.

Using the hill-climbing procedure, the error function based on Eq. 15 was used to determine the optimum value of each coefficient. The minimum value of the error function, which corresponds to the most optimal values of $L_{R_{(P)}(S)}$ and $\gamma_{R_{(P)}(S)}$, is plotted in the three-dimensional graph of Fig. 17.

$$J_{\text{Error}} = \frac{1}{T}\sum_{t=0}^{t=T}\left| F_{RY(S)} - \frac{1}{2}\rho S_{R(S)} F'_{RY(S)}(\alpha_{R(S)}) U_{R}^{2}{}_{(S)} \right| dt \quad (15)$$
$$(P) \qquad (P) \qquad (P) \qquad (P)$$

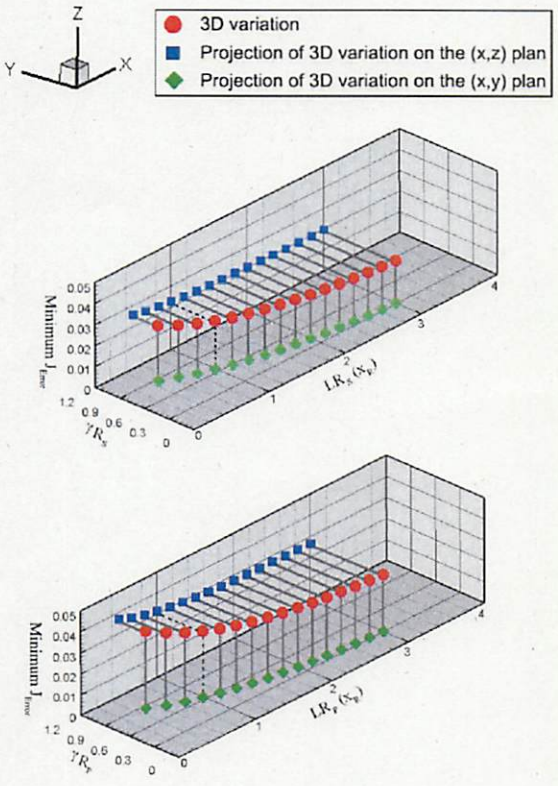

Fig. 17 Variation of $L_{R_{(P)}(S)}$, $\gamma_{R_{(P)}(S)}$ and error function J_{Error} from free-running experiments of the subject ship. Dotted lines refer to the optimum values of $L_{R_{(P)}(S)}$ and $\gamma_{R_{(P)}(S)}$

The variation of the optimum values is represented by the spherical shapes. The projections of the 3D variation on the (x, z) and (x, y) planes are respectively represented by square and diamond shapes. The minimum error function value does not significantly change for different increments of $L_{R_{(P)}(S)}$. The most suitable value that corresponds to the free-running experiment results corresponds to the one where $L_{R_{(P)}(S)} = x_{R_{(P)}(S)}$. However, there is a wide range of $\gamma_{R_{(P)}(S)}$ for different values of $L_{R_{(P)}(S)}$ where the error function is the minimum. Therefore, further optimization is carried out to determine $\gamma_{R_{(P)}(S)}$, while considering $L_{R_{(P)}(S)} = x_{R_{(P)}(S)}$.

Using the hill-climbing procedure, the value of $\gamma_{R_{(P)}(S)}$ for which J_{Error} is the minimum is selected as shown in Eq. 15. The variation of $\gamma_{R_{(P)}(S)}$ is shown in Fig. 18

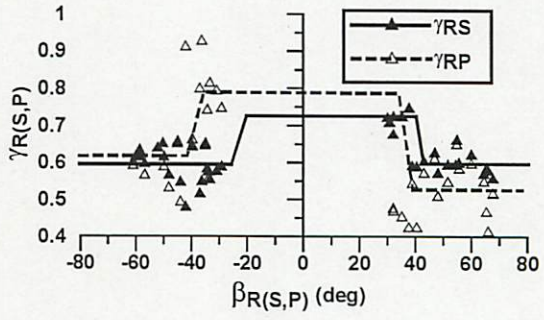

Fig. 18 Variation of $\gamma_{R_{(P)}(S)}$, $L_{R_{(P)}(S)} = x_{R_{(P)}(S)}$

5. SIMULATION OF FREE-RUNNING EXPERIMENTS

The validation of the MMG model developed for the subject ship will be conducted using free-running experiments. Free-running experiments were conducted at two different speeds U (initial speed) = 0.643m/s, rps = 7.97 and U (initial speed) = 1.029m/s, rps = 12.8, which correspond to the actual ship operating (5 knots) and cruising speed (8 knots) conditions. The experiment and simulation results of turning test for the rudder angles ($\delta_{(P)(S)} = \begin{Bmatrix} \pm 15^\circ \\ \pm 15^\circ \end{Bmatrix}$) at the ship's initial speed U= 0.643m/s is shown in Fig. 19.

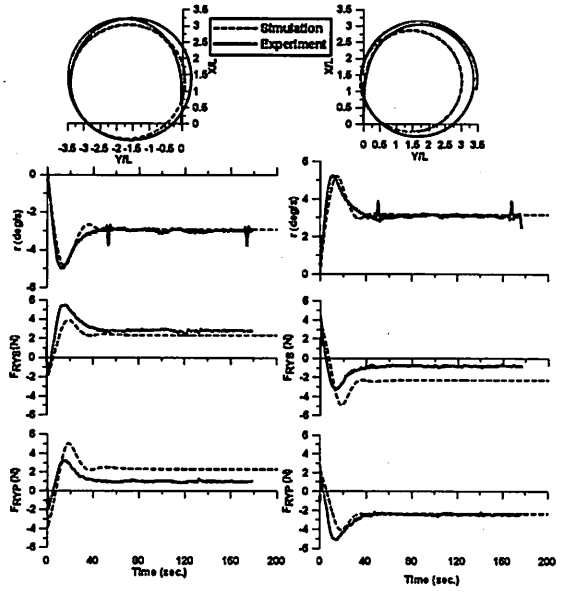

Fig. 19 Comparison between the free-running experiment and simulation results of the subject ship. LHS: $\delta_{(P)(S)} = \begin{Bmatrix} -15^\circ \\ -15^\circ \end{Bmatrix}$, RHS: $\delta_{(P)(S)} = \begin{Bmatrix} 15^\circ \\ 15^\circ \end{Bmatrix}$.

Initial speed U=0.643m/s, rps = 7.97

In this case, the outboard rudder (starboard rudder in port turning and port rudder in starboard turning) have opposite rudder normal force sign to the yaw rate and therefore to the turning direction. The proposed model can simulate the trend of the rudder force and the ship's yaw rate observed during experiments. During the turning motion, the normal force for inboard rudder (port rudder in port turning and starboard rudder in starboard turning) also has the opposite sign to the yaw rate and to the turning direction. It shows a lot more difference for inboard rudders between experiment and simulation. The free-running experiments and simulation results of turning test for the rudder angles ($\delta_{(P)(S)} = \begin{Bmatrix} \pm 35^\circ \\ \pm 35^\circ \end{Bmatrix}$) at the ship's initial speed U = 0.643m/s are shown in Fig. 20.

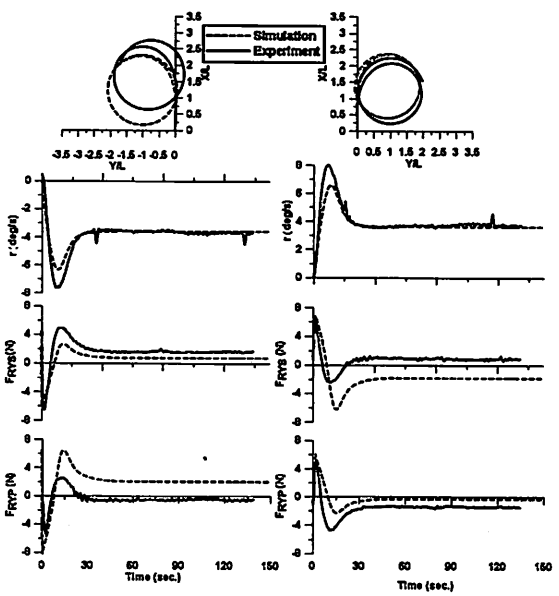

Fig. 20 Comparison between the free-running experiment and simulation results of the subject ship. LHS: $\delta_{(P)(S)} = \begin{Bmatrix} -35^\circ \\ -35^\circ \end{Bmatrix}$, RHS: $\delta_{(P)(S)} = \begin{Bmatrix} 35^\circ \\ 35^\circ \end{Bmatrix}$.

Initial speed U=0.643m/s, rps = 7.97

In this case, the inboard rudder has the same rudder normal force sign to the yaw rate and consequently to the turning direction. However, the outboard rudder has the opposite rudder normal force to the turning direction. The simulation can accurately capture the trend of the outboard rudder normal force. The difference between simulation and experiment for inboard rudder normal force is higher. The rudder normal force for port and starboard turns is slightly asymmetric, and the pattern of asymmetry is different from that of the SPTR system. The proposed model was used to simulate the rudder normal force for the zigzag experiments. The experiments and simulation results are shown in Fig. 21.

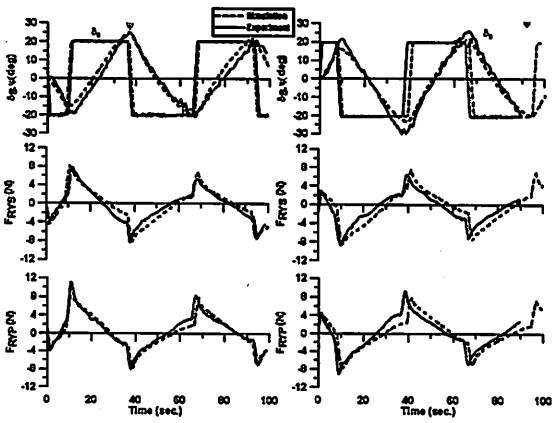

Fig. 21 Comparison between the free-running experiment and simulation results of the subject

ship. LHS: $\delta_{\substack{(S)\\(P)}} = \begin{Bmatrix} -20^\circ/-20^\circ \\ -20^\circ/-20^\circ \end{Bmatrix}$, RHS: $\delta_{\substack{(S)\\(P)}} = \begin{Bmatrix} 20^\circ/20^\circ \\ 20^\circ/20^\circ \end{Bmatrix}$. Initial speed U=0.643m/s, rps = 7.97

In this case, the direction of rudder normal force is opposite to the turning motion. The normal rudder normal force during a zigzag manoeuvre can be simulated very well. It can be concluded that when there is less nonlinearity, the proposed model works well.

For the subject ship, the axial distance between rudder and propeller is $\alpha_{R_{(P)}(S)} = 0.77\ D_{P_{(P)}(S)}$. For conventional ships, this value is $0.15 \sim 0.20\ D_P$ [11]. This may be contributing to the change in the direction of inflow to the rudder during manoeuvring motions, resulting in the non-conventional sign of rudder normal force phenomenon for the subject twin-propeller twin-rudder model ship. Further work in this direction is necessary to draw firm conclusions.

6. CONCLUSION

In this paper, the full mathematical model for manoeuvring of twin-propeller twin-rudder ship based on captive model tests and free-running experiments was established. Main conclusions are summarised as follows:

1- The effective wake-fraction for propeller inflow and the thrust deduction factor in straight ahead motion for the subject model ship show a constant variation with respect to the ship's advance ratio.

2- The coefficient x_H has almost constant value regardless the principal particulars of twin-propeller twin-rudder ships. The coefficient of reduction of rudder's resistance in ship's surge direction t_R seems to have a slight variation as compared with x_H's one. Whereas a_H has the most noticeable variation especially with respect to ships' block coefficients. Interestingly, the variation of a_H with respect to ships' block coefficients for twin-propeller twin-rudder ships shows a similar trend with the one for single-propeller single rudder ships [1].

3- An experiment-based method to estimate rudder-hull interaction coefficients from free-running experiments was proposed. The flow-straightening coefficient variation shows as slight asymmetric behaviour for starboard and port turning.

4- The opposite sign of the effective inflow angle as compared to the rudder angle during turning seems to be a typical twin-rudder ship phenomenon. For the subject twin-propeller twin-rudder model ship, the phenomenon seems to be quite significant and was observed for the entire range of rudder angle.

5- For twin-propeller twin-rudder system, the equivalent arm lever for sway motion is estimated to be as follows $L_{R_{(P)}(S)} = x_{R_{(P)}(S)}$.

REFERENCES

[1] Mathematical Modelling Group Report I, II, III, IV and V (1977, 1980) Bull Soc Nav Archit Jpn, 575: 192-198, 577: 322-329, 578:358-372, 579:404-413 and 616: 572–573 (in Japanese)

[2] Khanfir S, Nagarajan V, Hasegawa K et al. (2009) Estimation of mathematical model and its coefficients of ship manoeuvrability for a twin-propeller twin-rudder ship. In: Proceedings of MARSIM'09, Panama City, pp. M159-M166

[3] Khanfir S, Hasegawa K, Nagarajan V et al. (2011) Manoeuvring characteristics of twin-rudder systems: rudder-hull interaction effect on the maneuverability of twin-rudder ships. J Mar Sci Technol 16:472–490

[4] Lee SK, Fujino M, Fukasawa T (1988) A study on the manoeuvring mathematical model for a twin-propeller twin-rudder ship. J of Soc of Nav Archit of Jpn 163: 109-118 (in Japanese)

[5] Lee SK, Fujino M (2003) Assessment of mathematical model for the manoeuvring motion of a twin-propeller twin-rudder ship. Intl Ship Prog 50: 109-123

[6] Yoshimura Y, Sakurai H (1989) Mathematical model for the manoeuvring motion in shallow water (3rd report). J of The Kansai Soc of Nav Archit, Japan, 211: 115-126. (in Japanese)

[7] Kim YG, Kim SY, Kim HT et al. (2007) Prediction of the maneuverability of large container ship with twin propellers and twin rudders. J Mar Sci Technol 12:130–138

[8] http://www.ihi.co.jp/index-e.html

[9] Harvald SV AA (1983) Resistance and propulsion of ships. Wiley-interscience New York, USA. pp: 102-103.

[10] Personal discussions with Y. Toda, Osaka University, (2008).

[11] The Kansai Society of Naval Architects (1983), Japan, Zosen sekkei binran (Shipbuilding design handbook) (4th edn). Tokyo, pp:474-475 (in Japanese).